Reduction of Optical Beat Interference in Optical Frequency-Hopping CDMA Networks Using Coherence Multiplexing

Katsuhiro Kamakura and Iwao Sasase
Department of Information and Computer Science, Keio University
3-14-1 Hiyoshi, Kohoku, Yokohama, 223-8522 Japan

Abstract—**In order to reduce the optical beat interference (OBI) in an optical frequency-hopping code division multiple access (FH-CDMA) network, we propose applying coherence multiplexing (CM) technique into the optical FH-CDMA network. Since the CM technique achieves multiplexing by using time delays exceeding the coherence time of the light sources, crosstalk between CM channels depends on a space of delay difference between CM channels. We analyze the ratio of crosstalk to signal as a function of the space, and find a channel space enough to neglect crosstalk from other CM channels. Using this channel space, we obtain the number of CM channels accommodated within one chip duration. Since the conventional FH-CDMA supports traffic by the code channels only, its capacity is limited by OBI as traffic increases. In addition to the code channel, the proposed network supports traffic by the CM channels. Since the addition of CM channels decreases the number of active code channels for uniform traffic, OBI is reduced. Numerical results show that the proposed network attains larger capacity than the conventional FH-CDMA.**

I. Introduction

Optical code division multiple access (CDMA) has attracted great attention to meet the ever-growing needs of optical network with large capacity. The chief advantage of optical CDMA is random access capability. Optical CDMA also provides a great flexibility in a multiuser environment with bursty users. Most types of optical CDMA use the time domain for coding with optical delay lines and optical orthogonal codes [1]. Several alternatives use the frequency domain for coding with broadband light sources [2]. A new method with fiber Bragg gratings (FBGs) is introduced in [3]. FBGs have attracted great attention for devices in various applications of optical communications [4]. In [3], FBGs are coding devices, which slice the spectrum of the incoming pulse to reflect. The output of the devices is a train of pulses the frequencies of which are hopping in time. This type of optical CDMA is called optical frequency-hopping CDMA (FH-CDMA). It has an advantage of coding optically and passively.

In optical FH-CDMA, frequencies used in one active code channel are interfered by ones used in the other active code channels. This interference is called multiaccess interference, which causes crosscorrelation between codes assigned to code channels. The interference is reduced by the balanced detection to be very low level in [5], but capacity of optical FH-CDMA is susceptible to the number of active code channels. This susceptibleness arises due to light from incoherent sources interfering at the photodetectors. Owing to the square-law process of photodetection, the generated photocurrent contains cross-product terms, which produce broadband incoherent interference. This interference is called optical beat interference (OBI) [6]-[8]. OBI is caused by two of more lasers transmitting simultaneously on the same optical bandwidth. These extra components of the cross-product terms degrade a signal-to-noise ratio (SNR) in the code channel. This degradation induces channel outage, and limits the network capacity.

Similar problems have also been studied for subcarrier-multiplexed (SCM) networks [7]. In optical CDMA, an attempt to reduce OBI is made by using pulse position modulation (PPM) [8]. Since PPM confines transmitted power to a smaller fraction of each word interval, it allows to decrease the number of channels accessing at the same slot simultaneously. Thus, PPM leads to the decrease of the number of the cross-product terms caused at the photodetector. It is true that OBI is reduced as the number of slots in PPM, but the relative effects of dark current and thermal noises become large. This solution is not essential to reduce OBI, because there is a limit on increasing the number of slots. Optical FH-CDMA suffers from the limit similarly.

In this paper, we propose a coherence multiplexed FH-CDMA (CM/FH-CDMA) network to reduce OBI. CM technique uses time delays exceeding the coherence time of the light sources to achieve multiplexing, and is investigated in the field of telecommunication applications [5][9]. The advantage of no requirement of synchronization between CM channels does not spoil the random access capability of optical FH-CDMA. With the idea of adding new multiplexing channels in FH-CDMA, the proposed network reduces OBI. We call the new multiplexing channels CM channels. Considering the balanced detection in detail, we show that it rejects the common mode components of CM channels in the received signal. To add CM channels to FH-CDMA, we find a channel space enough to neglect crosstalk from other CM channels. Using this channel space, we obtain the number of CM channels accommodated within one chip duration. In this way, we apply CM channels to optical FH-CDMA, without increasing crosstalk between CM channels. Since the proposed network supports traffic by the CM channels as well as the code channels, the number of cross-products causing at the photodetector is decreased, and thus OBI is reduced. Numerical results show that the proposed network attains larger capacity than the conventional FH-CDMA.

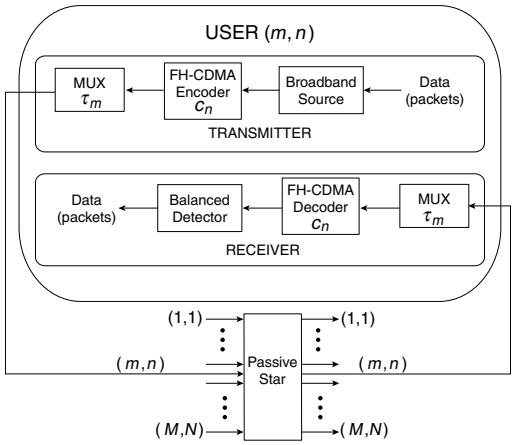

Fig. 1. A block diagram of the (m, n)th user in CM/FH-CDMA optical networks.

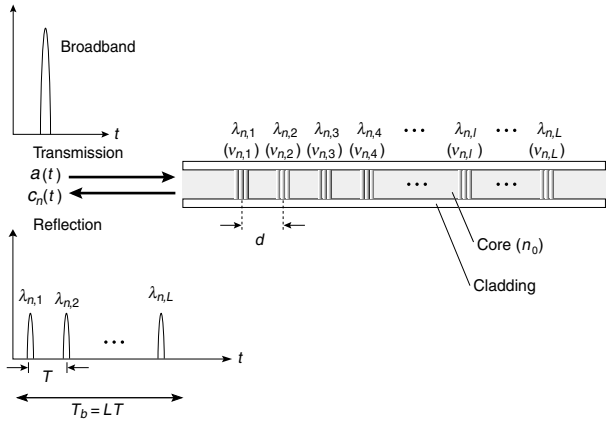

Fig. 2. The nth FH-CDMA encoder is shown, which are fiber Bragg gratings (FBGs) written for the Bragg wavelengths corresponding to $\lambda_{n,1}$, $\lambda_{n,2}$, $\ldots$, $\lambda_{n,L}$, corresponding to center frequencies $\nu_{n,1}$, $\nu_{n,2}$, $\ldots$, $\nu_{n,L}$, respectively.

II. CM/FH-CDMA Optical Networks

We describe the proposed CM/FH-CDMA network. Fig. 1 shows a general network configuration for implementing passive star networks. We consider a user labeled (m, n), where $m \in \{1, \ldots, M\}$ and $n \in \{1, \ldots, N\}$. The (m, n)th user has two pairs for accessing channels: one pair is a pair of coherence multiplexer (mux) and demultiplexer (dmux) that access the mth CM channel with delay τ_m, and another is a pair of the encoder and decoder that access the nth code channel with code c_n.

A. Encoder and Decoder Pairs

We describe the code channels. The coding device consists of a series of FBGs as shown in Fig. 2. The FBGs divide an available optical bandwidth $\Delta\nu$ into N frequency bins, each of which has a bandwidth $\Omega = \Delta\nu/N$. Each FBG has an index of refraction varying periodically along its length. It reflects a narrow wavelength, called Bragg wavelength λ_B. Each FBG is the bandpass filter with center frequency of c/λ_B, where c is the light speed. We denote the Bragg wavelengths of the FBGs by $\lambda_0, \ldots, \lambda_{N-1}$, corresponding to center frequencies $f_0, \ldots, f_{N-1}$, respectively. In the design of our network, important parameters are the Bragg wavelength λ_B, the grating length L_g, the grating period Λ, and the effective index of the fiber core n_0. A duration of a round-trip propagation through a grating is $T = 2n_0L_g/c$, which is defined to be a chip duration. The chip duration and the number of FBGs limit the bit duration T_b, because all reflected pulses should go out the FBGs before the next pulse's incoming. Since we assume that the encoder has ℓ FBGs at even intervals, T_b is given by $2n_0LL_g/c$. Furthermore, the encoder reflects ℓ out of N frequency bins according to c_n, which is assigned to the nth code channel. The center frequency of the ℓth FBG in the nth encoder is denoted by $\nu_{n,\ell}$, where $\nu_{n,\ell} \in \{f_0, \ldots, f_{N-1}\}$. Each of the reflected frequencies occupies a chip duration in the order of the position of the FBGs, and the resultant output of the FBGs is a train of pulses with ℓ hopping frequencies over a bit duration. The reflected pulse is assumed to be the inverse Fourier transform of the product between the incident pulse spectrum and the grating reflection response. Since we assume the light source to be broadband, the incident spectrum is reasonably flat over the grating response bandwidth Ω.

The transfer function of the ℓth FBG in the nth encoder is expressed as

$$H_{n,\ell}(\nu) = \mathrm{rect}\left(\frac{|\nu - \nu_{n,\ell}|}{\Omega}\right) e^{-i2\pi\nu\ell T}, \tag{1}$$

where $\mathrm{rect}(|\nu - \nu_{n,\ell}|/\Omega)$ is rectangular with center frequency $\nu_{n,\ell}$ and bandwidth Ω:

$$\mathrm{rect}(x) = \begin{cases} 1, & \text{for } |x| \le \dfrac{1}{2} \\ 0, & \text{otherwise.} \end{cases} \tag{2}$$

For simplicity of later analysis, we express the transfer function of the nth encoder as

$$H_n(\nu) = \sum_{l=1}^{L} H_{n,\ell}(\nu)\,. \tag{3}$$

B. Coherence Multiplexing

The mux and dmux consist of Mach-Zehnder interferometers (MZIs) with differential delays exceeding the coherence time of the light source τ_c. If the light source is assumed to have the rectangular spectrum with bandwidth $\Delta\nu$, then $\tau_c \simeq 1/\Delta\nu$ [11]. The output of the MZI is a sum of two fields with time delay τ_m. This operation denotes $\mathcal{L}_m[\boldsymbol{c}_n(t)]$, which splits, delays with τ_m, and recombines the encoded optical field $\boldsymbol{c}_n(t)$. The analytical signal of the transmitted signal is expressed as

$$\boldsymbol{s}_{m,n}(t) = \frac{\boldsymbol{c}_n(t) + \boldsymbol{c}_n(t - \tau_m)}{2} \equiv \mathcal{L}_m\big[\boldsymbol{c}_n(t)\big], \tag{4}$$

where bold typesets denote complex-valued signals in this paper.

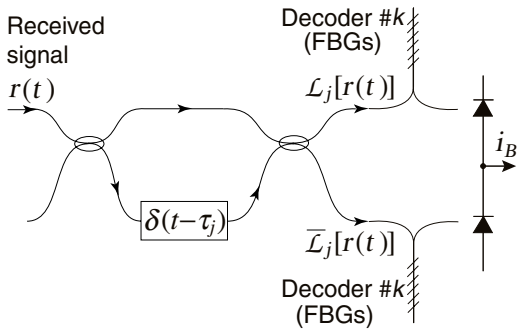

Fig. 3. The schematic diagram of the (j,k)th receiver based on the balanced detection is shown.

Let the Fourier transform of the operator $\mathcal{L}_m$ be $\mathcal{H}_m(\nu)$. We equivalently describe the mth MZI as a spectral operation that changes the spectrum of the optical fields over L chip durations. With the Wiener-Khinchin theorem, an equivalent expression of the MZI is given by

$$\mathcal{G}_{m,n}(\nu) = \left|\mathcal{H}_m(\nu)\right|^2 \sum_{l=1}^{L} \left|H_{n,l}(\nu)\right|^2 G_{m,n}(\nu)\,, \tag{5}$$

where $G_{m,n}(\nu)$ is the power spectrum density (psd) of the light source in the (m,n)th transmitter.

C. Receiver Description

Fig. 3 shows the schematic diagram of the (j,k)th receiver. The optical field received in the front of the (j,k)th receiver is given by

$$\begin{aligned}&\boldsymbol{r}(t)\\ &= \alpha \sum_m \mathcal{L}_m \left[\sum_n h_n(t-\zeta_{m,n}) \otimes \boldsymbol{a}_{m,n}(t-\zeta_{m,n}) \right], \end{aligned} \tag{6}$$

where $\otimes$ denotes the convolution, α is an attenuation coefficient to considering the splitting loss of the star coupler $1/(MN)$, and $\zeta_{m,n}$ is the relative delay of the (m,n)th signal. We consider $\zeta_{m,n} = \xi_{m,n}T$, $\xi_{m,n} \in \{0,\ldots,L-1\}$, because we assume the network to be chip-synchronous. We assume the (j,k)th receiver to be synchronous to the (j,k)th transmitter, i.e., $\zeta_{j,k} = 0$. The optical field at the (j,k)th receiver is then expressed as

$$\boldsymbol{r}_{j,k}(t) = h_k^*(t) \otimes \mathcal{L}_j[\boldsymbol{r}(t)]\,. \tag{7}$$

We assume that all optical sources are thermal, and that the output of the single-mode fiber is a thermal source with a psd equal to the sum of the psd's from transmitters. The psd of the upper photodetector of the balanced detector is given by

$$\begin{aligned}G'_{j,k}(\nu) = \alpha \left|H_k^*(\nu)\right|^2 \left|\mathcal{H}_j(\nu)\right|^2 \sum_m^M \sum_n^N \\ \left|\mathcal{H}_m(\nu)\right|^2 \left|H_n(\nu)\right|^2 G_{m,n}(\nu)\, e^{-i2\pi\nu\xi_{m,n}T}, \end{aligned} \tag{8}$$

where $\left|\mathcal{H}_j(\nu)\right|^2 \left|\mathcal{H}_m(\nu)\right|^2$ is

$$\begin{aligned}&\frac{1}{4}\Bigg[1 + \cos[2\pi\nu\tau_j] + \cos[2\pi\nu\tau_m] \\ &\quad + \frac{\cos[2\pi\nu(\tau_m+\tau_j)]}{2} + \frac{\cos[2\pi\nu(\tau_m-\tau_j)]}{2}\Bigg]. \end{aligned} \tag{9}$$

As for the lower photodetector of the balanced detector in the (j,k)th receiver, we define the operator for the lower output as

$$\overline{\mathcal{L}}_j\left[\boldsymbol{r}(t)\right] = \frac{\boldsymbol{r}(t) - \boldsymbol{r}(t-\tau_j)}{2}, \tag{10}$$

where the sign of minus is due to the phase shift on coupling. We express the Fourier transform of $\overline{\mathcal{L}}_j$ as $\overline{\mathcal{H}}_j(\nu)$. Substituting $\left|\overline{\mathcal{H}}_j(\nu)\right|^2 \left|\mathcal{H}_m(\nu)\right|^2$ for $\left|\mathcal{H}_j(\nu)\right|^2 \left|\mathcal{H}_m(\nu)\right|^2$ in (8), we obtain the psd of the photodetector, as

$$\begin{aligned}G''_{j,k}(\nu) = \alpha \left|H_k^*(\nu)\right|^2 \left|\overline{\mathcal{H}}_j(\nu)\right|^2 \sum_{m=1}^{M} \sum_{n=1}^{N} \\ \left|\mathcal{H}_m(\nu)\right|^2 \left|H_n(\nu)\right|^2 G_{m,n}(\nu)\, e^{-i2\pi\nu\xi_{m,n}T}, \end{aligned} \tag{11}$$

where $\left|\overline{\mathcal{H}}_j(\nu)\right|^2 \left|\mathcal{H}_m(\nu)\right|^2$ is

$$\begin{aligned}&\frac{1}{4}\Bigg[1 - \cos[2\pi\nu\tau_j] + \cos[2\pi\nu\tau_m] \\ &\quad - \frac{\cos[2\pi\nu(\tau_m+\tau_j)]}{2} - \frac{\cos[2\pi\nu(\tau_m-\tau_j)]}{2}\Bigg]. \end{aligned} \tag{12}$$

In (9) and (12), we note that the optical powers detected at both photodetectors have the common signal terms. They are canceled out by the balanced detection. Thus, the psd of the balanced detector in the (j,k)th receiver is given by

$$\begin{aligned}\widehat{G}_{j,k}(\nu) = \frac{\alpha\left|H_k(\nu)\right|^2}{4} \sum_{m=1}^{M} \sum_{n=1}^{N} \left|H_n(\nu)\right|^2 e^{-i2\pi\nu\xi_{m,n}T} \\ \cdot G_{m,n}(\nu)\big\{2\cos[2\pi\nu\tau_j] + \cos[2\pi\nu(\tau_m+\tau_j)] \\ + \cos[2\pi\nu(\tau_m-\tau_j)]\big\}. \end{aligned} \tag{13}$$

For simplicity, all the optical sources have the same spectrum $G_0(\nu)$, given by

$$G_0(\nu) = \frac{1}{\Delta\nu}\mathrm{rect}\left(\frac{\nu-\nu_0}{\Delta\nu}\right), \tag{14}$$

where ν_0 is the center frequency of the optical spectrum and $\Delta\nu$ is its bandwidth.

The optical power incident on the (j,k)th receiver is calculated by integrating $\hat{G}_{j,k}(\nu)$ over the frequency. We consider a power received from the (m,n)th source arriving at the (j,k)th receiver: we denotes it by $I_{m,n\to j,k}$. By taking one out of MN terms in (13),

$$\begin{aligned}I_{m,n\to j,k} = \frac{\alpha I_0}{4\Delta\nu} \sum_{l=1}^{L} \int_{\nu_{k,l}-\Omega/2}^{\nu_{k,l}+\Omega/2} \left|H_{n,l+\xi_{m,n}}(\nu)\right|^2 \\ \cdot \big\{2\cos[2\pi\nu\tau_j] + \cos[2\pi\nu(\tau_m+\tau_j)] \\ + \cos[2\pi\nu(\tau_m-\tau_j)]\big\} d\nu, \end{aligned} \tag{15}$$

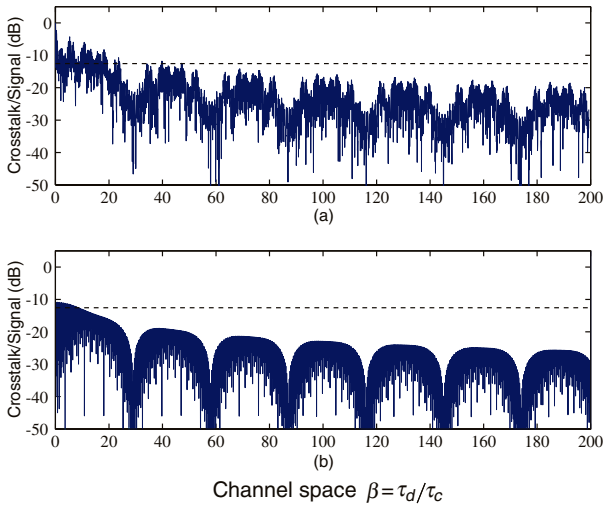

Fig. 4. Crosstalk from the adjacent CM channel as a function of channel space $\beta = \tau_d/\tau_c$, where $\tau_c = 1/\Omega$: (a) for the same code channel, (b) for the different code channel. The broken lines correspond to the ratio of the crosstalk to the signal is $1/18$.

where I_0 is the average power. Performing the integration, we get

$$I_{m,n\to j,k} = \frac{\alpha I_0 \Omega}{4\Delta\nu} \sum_{l=1}^{L} \delta\big(\nu_{k,l}, \nu_{n,l+\xi_{m,n}}\big) \cdot \left[2\,\mathrm{sinc}\left(\frac{\tau_j}{\tau_c}\right)\cos(2\pi\nu_{n,l}\tau_j) + \mathrm{sinc}\left(\frac{\tau_m+\tau_j}{\tau_c}\right)\cos[2\pi\nu_{n,l}(\tau_m+\tau_j)] + \mathrm{sinc}\left(\frac{\tau_m-\tau_j}{\tau_c}\right)\cos[2\pi\nu_{n,l}(\tau_m-\tau_j)] \right], \quad (16)$$

where $\mathrm{sinc}(x) = \sin(\pi x)/(\pi x)$, $\tau_c = 1/\Omega$, and $\delta(x, y)$ is the Kronecker delta function: the output is one if $x = y$, while it is zero if $x \neq y$.

Here, we describe the codes used in the network. For FH-CDMA, one-coincidence codes (OCCs) are studied. The OCCs have the following three characteristics: 1) all of code sequences have the same length, 2) each frequency is used at most once within a code sequence period, 3) the number of frequencies hitting between any pair of code sequences for any time shift equals one at most. Among OCCs, we use the family of OCCs generated by the algorithm studied in [10]. Hence, we consider that when $n \neq j$, $\delta\big(\nu_{k,l}, \nu_{n,l+\xi_{m,n}}\big)$ in (16) is at most one for l from 1 to L.

We assume that the CM channels are constructed by a unit delay τ_d, and that the mth CM channel has channel delay $\tau_m = m\tau_d$. Then we obtain a simple expression for crosstalk between CM channels. Crosstalk is dominated by two terms, which are due to two adjacent channels. The channel space between the desired CM channel and the adjacent CM channel is $\tau_d = |\tau_j - \tau_{j\pm1}|$: this is the worst case. Fig. 4 shows the ratio of crosstalk from the adjacent CM channel against signal as a function of the channel space $\beta = \tau_d/\tau_c$: (a) for the same code channel, and (b) for the different code channel, where $\Delta\nu = 10\,\mathrm{nm}$, $N = 29$, and $L = 12$. The broken lines correspond to the ratio of $1/18$, which guarantees the bit error rate of 10^{-9}. We see that crosstalk is negligible if β exceeds about 80, even though the same code channel with $\zeta_{m,k} = 0$ is active in the adjacent channel. In view of the rare case of $\zeta_{m,k} = 0$, $\beta = 80$ is enough for neglecting crosstalk. Suppose that $T = 10^{-9}\,\mathrm{s}$. Since we consider the fine unit delay to be $80\tau_c = 1.29 \times 10^{-10}\,\mathrm{s}$, the number of available CM channels becomes $T/80\tau_c \simeq 8$.

D. SNR Analysis

The (j, k)th receiver detects the intensity in the jth CM channel only when τ_m is congruent with τ_j. Note that the (j, k)th receiver is insensible to intensities in other CM channels. This insensibleness allows us to consider the third term only with $\tau_m = \tau_j$ in (16) to be the contributions to $\hat{G}_{j,k}(\nu)$. Since the detected signal results from optical interference, the magnitude is proportional to $\cos\phi_n$, where ϕ_n is the phase difference of the nth code channel relative to the kth code channel. For the matched code channel, the phase is stabilized to $\phi_k = 0$ in the upper photodetector, while in the lower photodetector $\phi_k = \pi$, reverting the polarity of the signal. For the desired signal, the control loop is stabilized to the point $\phi_k = 0$, while it is reconfigured to lock to the point $\phi_k = \pi$, reverting the polarity of the received data. The resulting photocurrent of the balanced detector is expressed as

$$i_B = \frac{\eta\alpha I_0 L\Omega}{4\Delta\nu}, \quad (17)$$

where η is the responsivity of the photodetector. Next, we consider the variance of the photocurrents. The variance of the photocurrent is given by [11]

$$\sigma_i^2 = \eta^2 T \int_{-\infty}^{\infty} \Lambda\Big(\frac{\tau}{T}\Big)\Gamma_I(\tau)\,d\tau - (\eta\bar{I}T)^2, \quad (18)$$

where $I(t)$ and $\bar{I}$ are the instantaneous power and the average power, respectively, and

$$\Lambda(x) = \begin{cases} 1-|x|, & \text{for } |x| \le 1 \\ 0, & \text{otherwise.} \end{cases} \quad (19)$$

Since we assume that all the sources are thermal with the same spectrum $G_0(\nu)$, for the case of a fully polarized field, we have

$$\Gamma_I(\tau) = \sum_n \eta^2 \bar{I}_n^2 \left[1 + |\gamma(\tau)|^2\right] + \eta^2 \sum_{v\neq w} \bar{I}_v \bar{I}_w \left[1 + |\gamma(\tau)|^2\right], \quad (20)$$

where $\gamma(\tau)$ is the complex degree of coherence of the light [11].

Let κ be the number of code channels hitting upon one frequency used in the desired code channel. The first term in (20) contains κ self products, while the second term has $\kappa(\kappa-1)/2$ possible pairs of cross-products. Since the average power with $n \neq j$ is $I_0\Omega/8\Delta\nu$, the variance given by (18) is reduced to

$$\sigma_i^2 = \frac{\kappa(\kappa+1)}{2T}\left(\frac{\alpha\eta I_0\Omega}{8\Delta\nu}\right)^2 \int_{-\infty}^{\infty} \Lambda\Big(\frac{\tau}{T}\Big)\,|\gamma(\tau)|^2\,d\tau. \quad (21)$$

Noting that the width of the function $\Lambda(\tau/T)$ is $2T$ whereas the width of the function $|\gamma_n(\tau)|^2$ is roughly twice the coherence time $2\tau_c$, we show that for $T \gg \tau_c$,

$$\frac{1}{T}\int_{-\infty}^{\infty}\Lambda\Big(\frac{\tau}{T}\Big)\,|\gamma_n(\tau)|^2\,d\tau \simeq \frac{\tau_c}{T}. \tag{22}$$

Since the light incident on each photodetector is from complementary spectral regions, the intensity noise from each photodetector is independent. Since we assume that data transmission is done by OOK, the average noise power is reduced by a factor of four. The variance of the photocurrent of the balanced detector is given by

$$\sigma_{i_B}^2 = \sigma_{i_{\rm up}}^2 + \sigma_{i_{\rm low}}^2 = \frac{(\alpha I_0)^2 B\kappa(\kappa+1)}{16\Delta\nu}, \tag{23}$$

where $B = 1/2T$ and $\Delta\nu = 1/\tau_c$.

With (17) and (23), the SNR is obtained as

$$\mathrm{SNR} = \frac{L^2\Delta\nu}{\kappa(\kappa+1)B}. \tag{24}$$

III. Network Performance

In this section, we evaluate throughput of the proposed network. The increase of active transmitters with the same delay τ_j leads to the increase of channels with the degraded SNR, because the SNR is a function of κ as derived in (24). Increasing the number of active code channels induces channel outage. For a packet network, the number of transmitters accessing the same CM channel increases with network load. Therefore, higher load increases the probability of channel outage, which in turn reduces throughput and capacity of the network. We consider a CM/FH-CDMA passive broadcast star network that guarantees chip-synchronous arrival of fixed-size packets. An ALOHA-type transmission scheme is applied: no sensing is done prior to transmission, and users retransmit packets under some predetermined protocol if a packet transmission is failed due to channel outage. We examine the basic limitation in the capacity of the proposed network corrupted by only the interference.

A. Throughput

We assume traffic to be uniform, where each user is equally likely to address any channel at any time. Since we assume no address contention, no more than one user is allowed to address a specific channel at a time. Using the SNR given by (24), we define channel outage as

$$\mathcal{I}_{\rm out}(L,\kappa,\Delta\nu,B) = \begin{cases} 1, & \text{for SNR} < Q \\ 0, & \text{for SNR} \geq Q, \end{cases} \tag{25}$$

where we set $Q = 22.5$, which is the value anticipated the bit error rate of 10^{-11}. We calculate the probability of channel outage by considering the traffic entering one receiver. Let the number of simultaneous users addressing the jth CM channel in one time slot be K. As mentioned in the previous section, no interference occurs between CM channels. Under the assumption of no address contention, K is bounded by 0 and N. Let the probability that a user transmits a packet in a time slot be ρ. Due to channel outage, the user has to retransmit more than once to send a packet successfully. Therefore, ρ is a measure of both new and retransmitted packets that are new packets entering the network with the same probability. Namely, we define the offered load as

$$G = KMq_n + (N-K)Mq_r = \rho MN, \tag{26}$$

where q_n and q_r are the probabilities of having a new packet and a retransmitted packet transmitted, respectively, at a given slot, and $q_n = q_r = \rho$. K has a binomial distribution

$$p(MN,K) = \binom{MN}{K}\rho^K(1-\rho)^{MN-K}. \tag{27}$$

Let the channel outage probability be $P_{\rm out}$. We described the dependence of SNR upon the number of code channels κ, the number of frequency bins N, optical bandwidth $\Delta\nu$, receiver bandwidth B. We define the probability that the desired code channel is practically interfered by κ code channels out of $\kappa - 1$ active other code channels, as

$$P_I(K,\kappa) = \binom{K}{\kappa}p_H^{\kappa}(1-p_H)^{K-\kappa}. \tag{28}$$

where p_H denotes the probability that one of frequencies used in the desired code channel is hit by one of frequencies used in other code channel. Then, with (25), (27), and (28), $P_{\rm out}$ is given by

$$P_{\rm out}(\rho\,|N,K,\Delta\nu,B) = \sum_{j=1}^{\min\{K,N\}} p(MN-1,j-1) \cdot \sum_{\kappa=1}^{j} P_I(j,\kappa)\,\mathcal{I}_{\rm out}(L,\kappa,\Delta\nu,B). \tag{29}$$

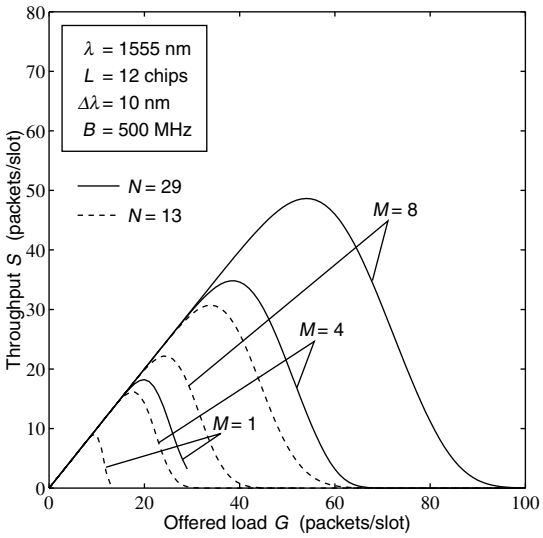

Fig. 5. The throughput S versus the offered load G for different values of M and N: $\Delta\lambda = 10\,\mathrm{nm}$ ($\Delta\nu = 620\,\mathrm{GHz}$), and $B = 500\,\mathrm{MHz}$.

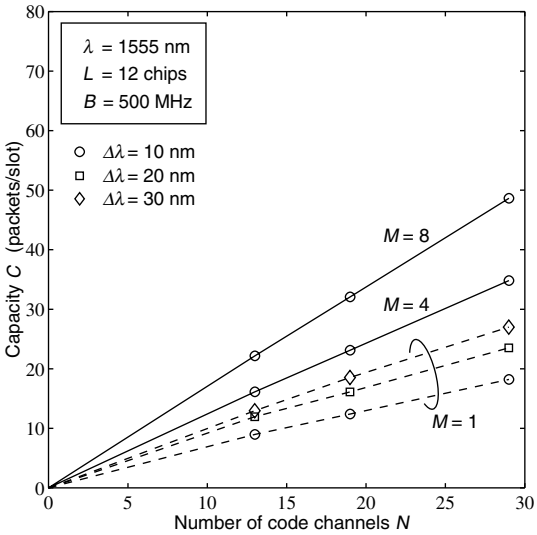

Fig. 6. The maximum capacity $C_{\max}$ is shown as a function of the number of code channels N used in the CM/FH-CDMA networks: $M = 1$, 4, and 8, $\Delta\lambda = 10\,\mathrm{nm}$ ($\Delta\nu = 620\,\mathrm{GHz}$), and $B = 500\,\mathrm{MHz}$.

Thus, with $G = \rho MN$, throughput is expressed as

$$S = 1 - G \cdot P_{\mathrm{out}}(\rho)\,. \tag{30}$$

Fig. 5 shows throughput S versus the offered load G for different values of M and N, provided $\Delta\lambda = 10\,\mathrm{nm}$ and $B = 500\,\mathrm{MHz}$. $M = 1$ corresponds to the conventional FH-CDMA. Wee see that for small G, S increases linearly with G. This is because there are few retransmissions. Since the effect of OBI is small for small G, few channel outages occur. As G increases, OBI becomes more frequent, and more retransmissions occur. For the conventional network ($M = 1$) with $N = 29$, throughput reaches its maximum when G is about 20, and the network cannot simply support the input traffic when G is beyond 20. Namely, there is the optimum G_{opt} that maximizes throughput S. This is because too many retransmissions occur due to channel outage: the SNR frequently falls below the setting Q-value in the region beyond G_{opt}. On the other hand, for the proposed network ($M = 4$ and 8), although throughput falls when G exceeds G_{opt}, the optimum G_{opt} is larger than that of the conventional network ($M = 1$). This is because OBI is reduced in the proposed network. Although the effect of OBI increases with the square of the number of transmitting lasers in the same CM channel as derived in (23), the proposed network supports the entering traffic by dividing it into M CM channels for a certain value of G. Because the number of active code channels per CM channel is then reduced, the OBI is reduced. Thus, the addition of CM channels leads the network to increase its throughput. We also see from Fig. 5 that the network with large N has larger throughput than that with small N.

The maximum throughput in the network is defined as capacity C. Fig. 6 shows capacity C as a function of the number of code channels N used in the proposed network. For reference, capacity of the conventional networks with $\Delta\lambda = 20\,\mathrm{nm}$ and $30\,\mathrm{nm}$ is shown. Using sources with large $\Delta\lambda$ is a method reducing OBI, but the proposed network has larger capacity than the network with such a method. The value of C can also be interpreted as the effective number of simultaneous channels. It follows that large M leads the network to increase its capacity.

IV. Conclusions

We have proposed the CM/FH-CDMA network to reduce OBI in optical FH-CDMA. Considering the balanced detector in detail, we show that it rejects the common mode components in the received signal. We find the channel space enough to neglect crosstalk between CM channels. The proposed network supports traffic by dividing it into CM channels. Then, the addition of CM channels decreases the number of cross-products causing at the photodetector, and thus, reduces OBI. Numerical results show that the proposed network enhances capacity of the conventional FH-CDMA for uniform traffic.

Acknowledgments

This research work was supported in part by NTT DoCoMo Inc.

References

[1] F. R. K. Chung, J. A. Salehi, and V. K. Wei, "Optical orthogonal codes: design, analysis, and applications," *IEEE Trans. Inform. Theory*, vol. IT-35, pp. 595–604, May 1989.

[2] H. P. Sardesai, C.-C. Chang, and A. M. Weiner, "A femtosecond code-division multiple-access communication system test bed," *J. Lightwave Technol.*, vol. 16, no. 11, pp. 1953–1964, Nov. 1998.

[3] H. Fathallah, L. A. Rusch, and S. LaRochelle, "Passive optical fast frequency-hop CDMA communications system," *J. Lightwave Technol.*, vol. 17, no. 3, pp. 397–405, Mar. 1999.

[4] K. O. Hill and G. Meltz, "Fiber bragg grating technology fundamentals and overview," *J. Lightwave Technol.*, vol. 15, no. 8, pp. 1263–1274, Aug. 1997.

[5] R. A. Griffin, D. D. Sampson, and D. A. Jackson, "Coherence coding for photonic code-division multiple access networks," *J. Lightwave Technol.*, vol. 13, no. 9, pp. 1826–1837, Sep. 1995.

[6] M. Nazarathy, W. V. Sorin, D. M. Baney, and S. A. Newton, "Spectral analysis of optical mixing measurements," *J. Lightwave Technol.*, vol. 7, no. 7, pp. 1083–1096, July 1989.

[7] M. M. Banat, and M. Kavehrad, "Reduction of optical beat interference in SCM/WDMA networks using pseudorandom phase modulation," *J. Lightwave Technol.*, vol. 12, no. 10, pp. 1863–1868, Oct. 1994.

[8] E. D. J. Smith, R. J. Blaikie, and D. P. Taylor, "Performance enhancement of spectral-amplitude-coding optical CDMA using pulse-position modulation," *IEEE Trans. Commun.*, vol. 46, no. 9, pp. 1176–1185, Sep. 1998.

[9] D. A. Blair and G. D. Cormack, "Optimal source linewidth in a coherence multiplexed optical fiber communications system," *J. Lightwave Technol.*, vol. 10, no. 6, pp. 804–810, Jun. 1992.

[10] L. Bin, "One-coincidence sequences with specified distance between adjacent symbols for frequency-hopping multiple access," *IEEE Trans. Commun.*, vol. 45, no. 4, pp. 408–410, Apr. 1997.

[11] J. W. Goodman, *Statistical Optics*, New York: John Wiley & Sons, Inc.